

Computational Quantum Chemical, Structural and Biological Studies on Uracil-5-Tertiary Sulfonamides

ABSTRACT

Aims: To study Computational Quantum Chemical (CQC), Pharmacokinetic and other biological components are listed in pairs of Uracil-5-Tertiary Sulfonamides "5- (4- (2,3-dihydrobenzo [b] [1,4] dioxine-2-carbonyl) piperazin -1-yl) sulfonyl) pyrimidine-2,4 (1H, 3H) -dione "(I) and" N-butyl-N-methyl-2,4-dioxo-1,2,3,4 -tetrahydropyrimidine-5 -sulfonamide "(II).

Methodology: FT-IR, FT-Raman, NMR (^1H , ^{13}C) and UV-Vis spectral chemical data were calculated and reported. DFT values for both combinations (I and II) were calculated using B3LYP / 6-31 + G (d, p) and B3LYP / 6-311 + G (2d, p). NMR chemical modification was calculated using the independent atomic orbital measurement method (GIAO). UV-Vis display is also calculated using the same basic sets.

Conclusion: The limits of Hyperpolarizability, HOMO and LUMO are listed. Pharmacokinetic properties (ADMET), drug similarity, bioactivity score, logP, pKa calculated using Molinspiration, pkCSM, Swiss ADME, Chem Axon.

Keywords: CQC, Pharmacokinetic, drug likeness, bioactivity score, Molinspiration and Chem Axonsoftware.

1. INTRODUCTION

Uracil derivatives in general and 5-Fluorouracil (5-FU) in particular are an antimetabolite used in the treatment of gastric tract/breast/liver cancer. [1]. The N1-substituted derivatives, nucleoside analog of 5- iodouracil and 5-trifluoromethyluracil show antiviral activity. N1 N3-disubstituted uracils possesses antibacterial and antifungal activities.

The synthesis and characterization of "5-(4-(2,3-dihydrobenzo[b][1,4]dioxine-2-carbonyl)piperazin-1-yl)sulfonyl)pyrimidine-2,4(1H,3H)-dione" (I) and "N-butyl-N-methyl-2,4-dioxo-1,2,3,4-tetrahydropyrimidine-5-sulfonamide" (II) and their characterization as well as activity studies have been reported by Sasidhar [2]. In this paper the results of the Computational Quantum Chemical studies, Pharmacokinetic and other physicochemical properties have been discussed and compared with the experimental result of sasidhar.

Materials and methods:

Computational details: The DFT calculations have been carried out with Gaussian 16 software package [3]. Geometrical optimization of compounds have been carried out with B3LYP exchange correlation functional with 6-31+G (d, p), 6-311+G (2d, p) basis set. For visualization in cases when Gaussian 16 software package was used, the Gauss View 6 program was employed [4]. The theoretical NMR (^1H and ^{13}C) chemical shifts were obtained at B3LYP/6-31+G (d, p), B3LYP/6-311+G (2d, p) level of theory, employing the GIAO

method, while the Dimethyl sulfoxide (DMSO) was considered as standard reference. Using TD-DFT CAM-B3LYP/6-311+G (2d, p) basis level, theoretical absorption wavelengths (λ), oscillator strengths (f) and major contributions to electronic transition were calculated in DMSO as solvent (SMD model). Biological aspects like Absorption, Distribution, Metabolism, Excretion, Toxicity, Physicochemical properties, Lipophilicity, Pharmacokinetics, Drug likeness were carried out by using Molinspiration[5,6], pkCSM[7], SwissADME[8,9] and Chemaxon[10] tools.

Results and discussion:

Molecular Geometry: The optimized geometrical parameters of both the compounds have been computed by DFT/B3LYP 6-31+G (d, p), DFT/B3LYP 6-311+G (2d, p) level of theory. The input and optimized geometries with the labelling of atoms are presented in Fig. 1 and 2. In this work, computations have been done in the gas phase and solvent phase. Infrared, ^1H and ^{13}C NMR results obtained in DFT calculations have been compared with the experimental results of sasidhar[2].

DFT calculations were performed with the Gaussian 16 package package [3]. The optimization of geometrical compounds was performed with B3LYP exchange functional correlation with 6-31 + G (d, p), 6-311 + G (2d, p) basis set. To visualize situations where the Gaussian 16 software package was used, the Gauss View 6 program was hired. [4] NMR (^1H and ^{13}C) chemical mutations were obtained at B3LYP / 6-31 + G (d, p), B3LYP / 6-311 + G (2d, p) theoretical level, using the GIAO method, while Dimethyl Sulfoxide (DMSO) was considered a standard reference. TD-DFT CAM-B3LYP / 6-311 + G (2d, p) level base, theoretical absorption wavelengths (λ), oscillator power (f) and major contributions to electronic conversion are listed in DMSO as solvent (SMD model). Biological factors such as Absorption, Distribution, Metabolism, Excretion, Toxicity, Physicochemical properties, Lipophilicity, Pharmacokinetics, Drug likeness are performed using Molinspiration [5,6], pkCSM [7], SwissADME [8,9] and Chemaxon [10] tools.

Discussion:

Molecular Geometry: The geometric parameters for both chemicals are calculated by DFT / B3LYP 6-31 + G (d, p), DFT / B3LYP 6-311 + G (2d, p) level of theory. Input and fine-tuned geometries have an atomic label shown in Fig. 1 and 2. In this work, calculations were performed on the gas and solvent phases. Infrared results, ^1H and ^{13}C NMR obtained in DFT calculations were compared with sasidhar test results [2].

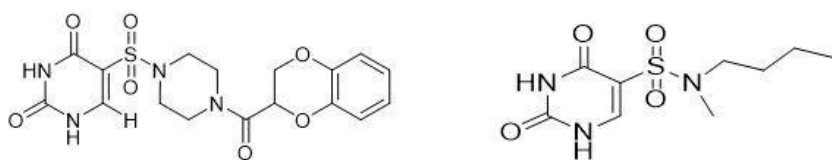


Fig.1: Input structure of 5-(4-(2,3-dihydrobenzo[b][1,4]dioxine-2-carbonyl)piperazin-1-yl)sulfonylpyrimidine-2,4(1H,3H)-dione and N-butyl-N-methyl-2,4-dioxo-1,2,3,4-tetrahydro pyrimidine-5-sulfonamide

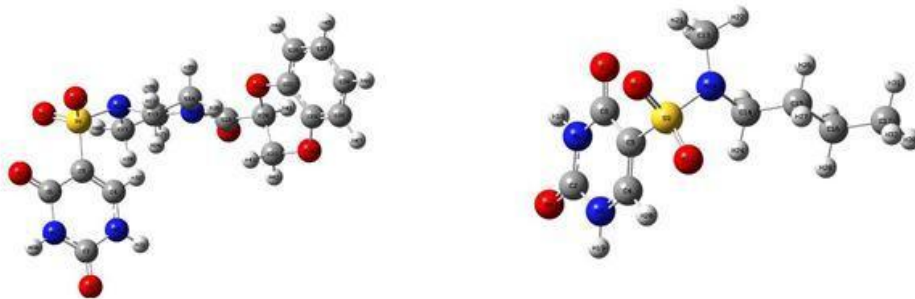


Fig. 2: The optimized geometrical structure of 5-(4-(2,3-dihydrobenzo[b][1,4]dioxine-2-carbonyl)piperazin-1-yl)sulfonylpyrimidine-2,4(1H,3H)-dione and N-butyl-N-methyl-2,4-dioxo-1,2,3,4-tetrahydropyrimidine-5-sulfonamide in solvent phase

Vibrational assignments: The experimental vibrational spectra (FT-IR) have been in comparison with the theoretically received spectra. Compounds I and II encompass forty seven atoms and 220 electrons, 32 atoms, and 138 electrons. Fig. three and four constitute the theoretical and experimental FT-IR spectra of each the compounds respectively. The experimental (FT-IR) measurements, computed vibrational (unscaled and scaled) wavenumbers, entire essential vibrational modes are supplied in Tables 1 and 2. Due to the correlation results of electrons and foundation set inadequacy, the experimental wavenumbers are usually decrease than the computed wavenumbers. For this reason, calculated wavenumbers are scaled with a scaling component of 0.933. The prediction of Raman intensities the Raman scattering activities (Si) changed into calculated with the GAUSSIAN sixteen software and the values are tabulated and the spectrum received is represented in Fig.5 and 6.

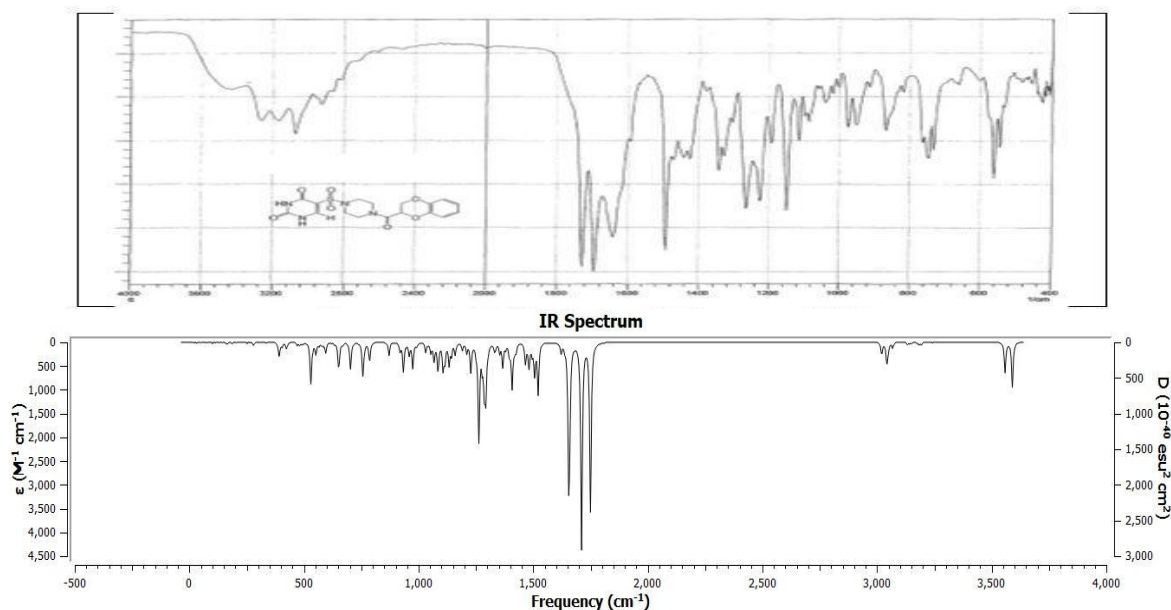
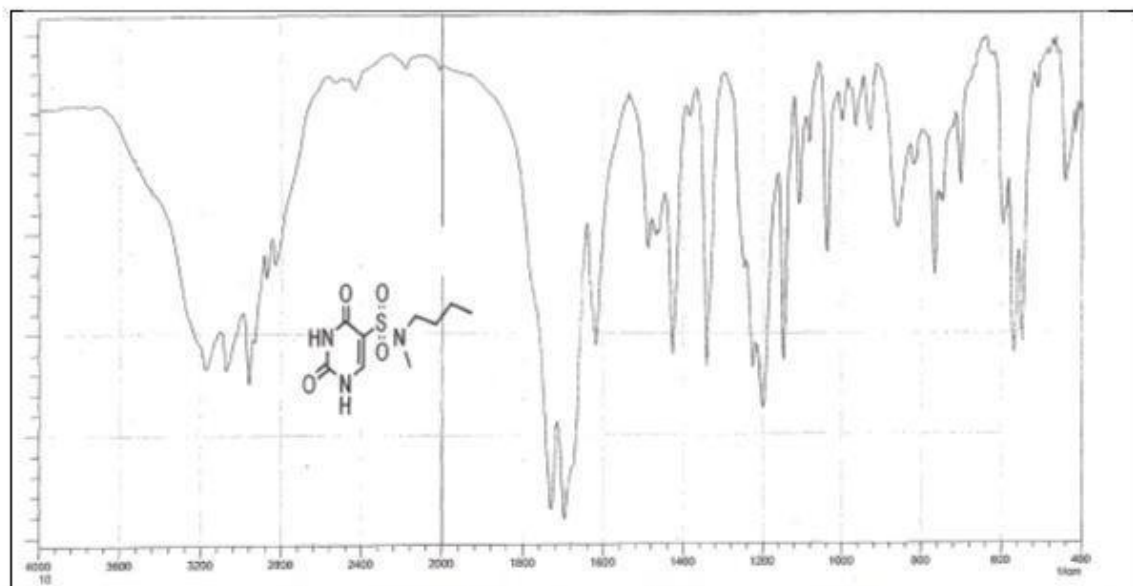


Fig. 3: Experimental and Theoretical FT-IR spectra of 5-(4-(2,3-dihydrobenzo[b][1,4]dioxine-2-carbonyl)piperazin-1-yl)sulfonylpyrimidine-2,4(1H,3H)-dione



IR Spectrum

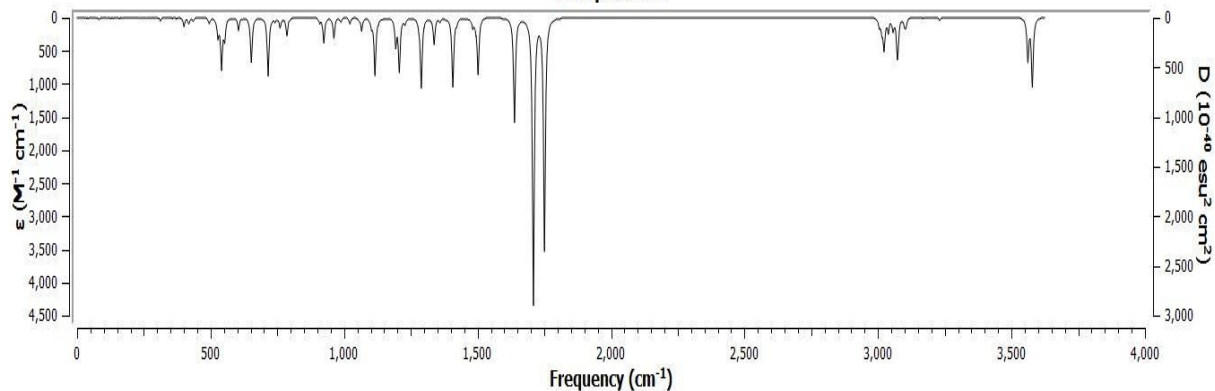


Fig. 4: Experimental and Theoretical FT-IR spectra of N-butyl-N-methyl-2, 4-dioxo-1, 2, 3, 4-tetrahydropyrimidine-5-sulfonamide

Raman Activity Spectrum

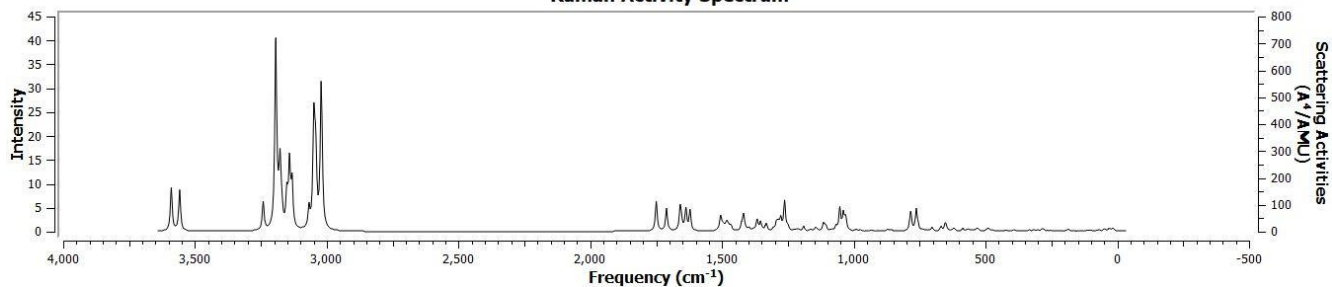


Fig. 5: Computational Raman spectra of 5-(4-(2,3-dihydrobenzo[b][1,4]dioxine-2-carbonyl)piperazin-1-yl)sulfonylpyrimidine-2,4(1H,3H)-dione

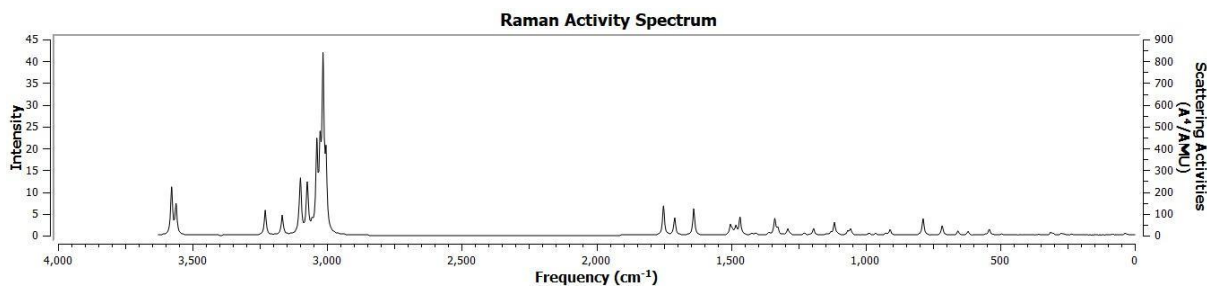


Fig. 6: Computational Raman spectra of N-butyl-N-methyl-2, 4-dioxo-1, 2, 3, 4-tetrahydropyrimidine-5-sulfonamide

N-H vibrations: The heteroaromatic shape suggests the presence of N-H stretching vibration above 3000cm⁻¹, that is the function area for prepared identity of this shape. These are the standard variety for CH₃, NH₂ and C-H vibrations. The N-H stretching vibration takes place within the area 3500-3200cm⁻¹. For compound I the scaled N-H stretch turned into calculated at 3359cm⁻¹ with the aid of using B3LYP/6-31G(d,p) fueloline section, at 3331cm⁻¹ with the aid of using B3LYP/6-31G+(d,p) solvent phase and 3319cm⁻¹ B3LYP/6-311G+(2d,p) solvent section, at 3346cm⁻¹ by B3LYP/ 6-311G+(2d,p) fueloline section and the experimental values discovered at 3280cm⁻¹ in FT-IR spectrum. The stretching vibration takes place within the area 3500-3200cm⁻¹. For compound II the scaled N-H stretch turned into calculated at 3359cm⁻¹ with the aid of using B3LYP/6-31G(d,p) fueloline section, at 3334cm⁻¹ with the aid of using B3LYP/6-31G+(d,p) solvent section and 3322cm⁻¹ B3LYP/6-311G+(2d,p) solvent section, at 3347cm⁻¹ with the aid of using B3LYP/ 6-311G+(2d,p) fueloline section and the experimental values discovered at 3200cm⁻¹ in FT-IR spectrum.

The theoretically values with the aid of using B3LYP/6-31G (d,p) and B3LYP/6-311+G(2d,p) strategies display superb settlement with the recorded experimental values. C-H vibrations: In fragrant compounds, the C-H stretching wavenumbers seem within the variety 3100–3000cm⁻¹ that is the function area for the prepared identity of C-H stretching vibrations [11]. In this area, the bands have been now no longer affected notably with the aid of using the character of substituent.

The C-H stretching modes normally seem with sturdy Raman depth and are enormously polarized. The theoretically computed values for compound I at 3018cm⁻¹ with the aid of using B3LYP/6-31G(d,p) fueloline section, at 3049cm⁻¹ with the aid of using B3LYP/6-31G+(d,p) solvent section, 3024cm⁻¹ with the aid of using B3LYP/6-311G+(2d,p) solvent section and at 2977cm⁻¹ with the aid of using B3LYP/ 6-311G+(2d,p) fueloline section and the experimental values discovered at 3180cm⁻¹ and for compound II the theoretically computed values at 2904cm⁻¹ with the aid of using B3LYP/6-31G(d,p) fueloline section, at 2915cm⁻¹ with the aid of using B3LYP/6-31G+(d,p) solvent section, 2896cm⁻¹ with the aid of using B3LYP/6-311G+(2d,p) solvent section and at 2887cm⁻¹ with the aid of using B3LYP/ 6-311G+(2d,p) fueloline section and the experimental values discovered at 3100cm⁻¹ in FT-IR spectrum approach proven exact settlement with experimental observations.

C=O Vibrations: The C=O stretching vibration is Raman and IR active. It is medium at 1600 cm⁻¹ and really susceptible at 1111 cm⁻¹ in IR. The computed values of compound I are discovered at 1695, 1649, 1632 and 1678cm⁻¹ respectively for B3LYP/6-31G(d,p) fueloline section, B3LYP/6-31G+(d,p) solvent section, B3LYP/6-311G+(2d,p) solvent section and B3LYP/ 6-311G+(2d,p) fueloline section at mode 117 and 1667, 1613, 1596 and 1651cm⁻¹ respectively for in B3LYP/6-31G(d,p) fueloline section, B3LYP/6-31G+(d,p) solvent section, B3LYP/6-311G+(2d,p) solvent section and B3LYP/ 6-311G+(2d,p) fueloline section at mode 116.

The experimental values for those modes are 1720cm⁻¹ and 1700 cm⁻¹ respectively. The computed values of compound II are discovered at 1693, 1651, 1633 and 1676cm⁻¹

respectively for B3LYP/6-31G(d,p) fueloline section, B3LYP/6-31G+(d,p) solvent section, B3LYP/6-311G+(2d,p) solvent section and B3LYP/ 6-311G+(2d,p) fueloline section at mode seventy five and 1651,1610,1594 and 1634cm⁻¹ respectively for B3LYP/6-31G(d,p) fueloline section, B3LYP/6-31G+(d,p) solvent section, B3LYP/6-311G+(2d,p) solvent section and B3LYP/ 6-311G+(2d,p) fueloline section at mode 74. The experimental values for those modes are 1720 and 1680 cm⁻¹ respectively. This C=O vibration produces a big quantity without cost electrons and this area of the molecule is extra bioactive with the human proteins and acts as a drug.

C=C Vibrations: The C=C fragrant stretching vibration offers upward thrust to function bands in each the discovered FT-IR spectra, protecting the spectral variety from 1600-1400cm⁻¹ [12]. Therefore, the C=C stretching vibrations for compound I were discovered in FT-IR spectrum at 1640cm⁻¹ have been assigned to C=C stretching vibration. The theoretically computed anharmonic frequencies at 1556cm⁻¹ with the aid of using B3LYP/6-31G(d,p) fueloline section, at 1554cm⁻¹ with the aid of using B3LYP/6-31G+(d,p) solvent section, 1543cm⁻¹ with the aid of using B3LYP/6-311G+(2d,p) solvent section and at 1551cm⁻¹ with the aid of using B3LYP/ 6-311G+(2d,p) fueloline section approach and the C=C stretching vibrations for the compound II were discovered in FT-IR spectrum at 1440cm⁻¹ have been assigned to C=C stretching vibration. The theoretically computed anharmonic frequencies at 1546cm⁻¹ with the aid of using B3LYP/6-31G(d,p) fueloline section, at 1533cm⁻¹ with the aid of using B3LYP/6-31G+(d,p) solvent section, 1528cm⁻¹ with the aid of using B3LYP/6-311G+(2d,p) solvent section and at 1541cm⁻¹ with the aid of using B3LYP/ 6-311G+(2d,p) fueloline section approach confirmed an awesome settlement with experimental data.

Non Linear Optical Properties: Organic NLO substances are determined withinside the vanguard of contemporary studies in substances science. In those regards, the NLO houses of each the compounds have additionally been addressed with the aid of using the DFT calculations of polarizability and primary order hyperpolarizability (Parallel & Perpendicular), Energy and Dipole second.

The houses like Electric dipole second, polarizability and primary order hyper polarizability (μ , α , Δ and β) for compound I and compound II are expressed. In Gaussian output, NLO houses are in atomic devices (a.u). These are transformed to conventional devices with the aid of using the use of 1 a. u. = 8.63x10⁻³⁰esu for β , 1 a. u = 2.fifty four Debye for μ and 1 a. u. = 0.15x10⁻²⁴esu for α [13]. The general static dipole second (μ), the imply polarizability (α), the anisotropy of the polarizability (Δ), the imply first-order hyperpolarizability (β) of each the compounds are summarized in Table 3.

The urea molecule has been taken into consideration as a prototypical molecule in terms of the NLO houses, for that reason the acquired computational consequences had been as compared with the urea. In order compare, calculations of NLO houses for urea molecule had been carried out on the equal stage of principle as for each the compounds. Computed dipole second is 3.2 D, that is extensively decrease than for the urea's dipole second of 3.89D. The static polarizability and primary order hyperpolarizability of each the compounds are determined to be 21.68x10⁻²⁴ to 29.seventy eight x10⁻²⁴ and 0.41x10⁻³⁰ to 0.45x10⁻³⁰, respectively, in esu devices. The end is that hyperpolarizability is sort of 0.seventy five instances than urea (β_{tot} = 0.62x10⁻³⁰esu).

NMR Observations: To decide the shape of natural compounds, the chemical shifts are usually used. They are commonly used for correct size of magnetic houses. The theoretical NMR (1H and 13C) chemical shifts are acquired at B3LYP/6-31G+(d,p) and B3LYP/6-311G+(2d,p) stage of principle, using the GIAO approach, even as the Dimethyl sulfoxide (DMSO) taken into consideration as popular reference. The theoretical NMR (1H and 13C) spectra are as compared with experimental NMR (1H and 13C) spectra and chemical shifts are offered in Table four to 7. In 13C NMR, the carbon atoms withinside the fragrant ring have chemical shifts withinside the variety of 106-143 and 104-143 ppm. The carbon atoms connected to the oxygen atom with the aid of using double bond withinside the variety of 134-143ppm [14, 15]. In each the compounds chemical shift values of carbon atoms

withinside the fragrant ring had been experimentally discovered withinside the variety of 149- one hundred sixty five and 111-159ppm. These values are in exact settlement with experimental consequences. The C2 atom is connected to the oxygen atom with the aid of using double bond is experimentally discovered at 143 and a hundred and fifty ppm. The chemical shifts of fragrant protons are regarded withinside the variety of 6.9-7.1and 7.95ppm. The Uracil protons of the hoop shape, those chemical shifts are experimentally discovered at 11.four ppm, while those alerts are theoretically acquired at 8.03 and 8.20 ppm. This end result is in exact settlement with literature [16]. All calculated NMR (1H, 13C) chemical shift values are in exact settlement with the experimental discovered values.

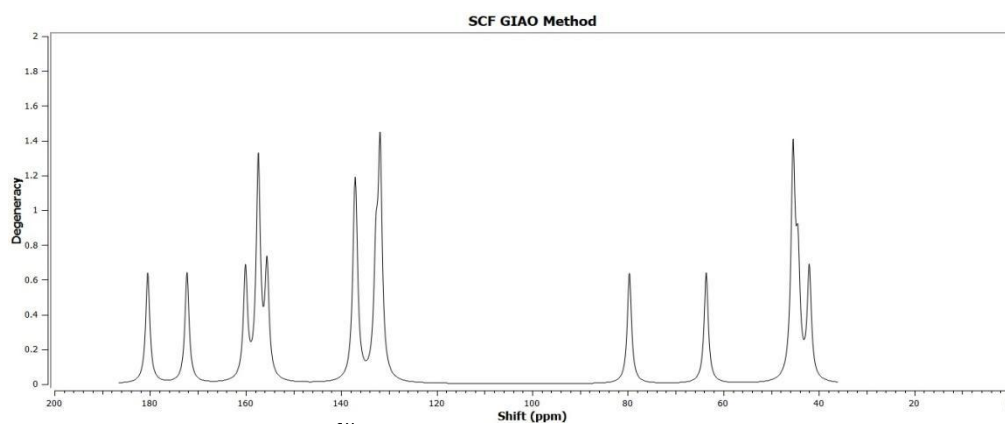


Fig. 7: Computational ^{13}C NMR spectra of 5-(4-(2,3-dihydrobenzo[b][1,4]dioxine-2-carbonyl)piperazin-1-yl)sulfonylpyrimidine-2,4(1H,3H)-dione

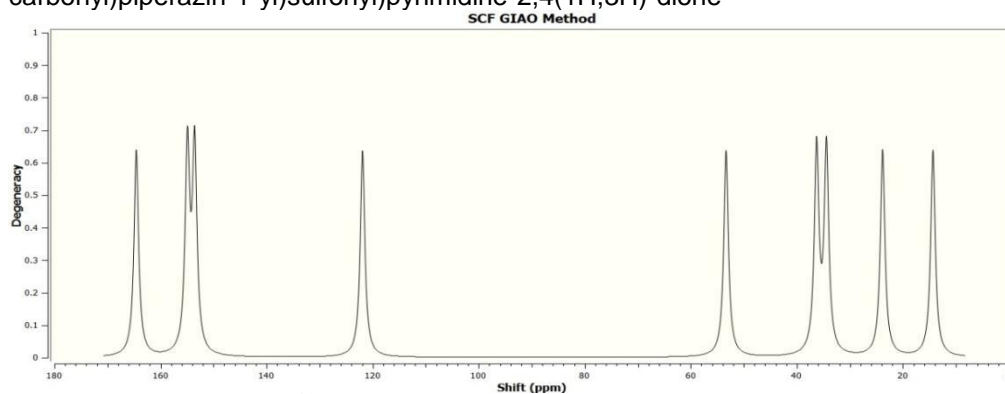


Fig. 8: Computational ^{13}C NMR spectra of N-butyl-N-methyl-2,4-dioxo-1,2,3,4-tetrahydropyrimidine-5-sulfonamide

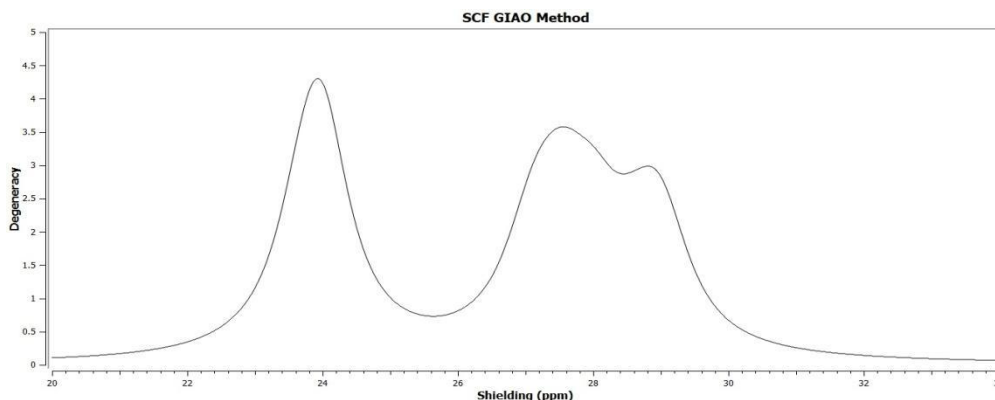


Fig. 9: Computational ^1H NMR spectra of 5-(4-(2,3-dihydrobenzo[b][1,4]dioxine-2-carbonyl)piperazin-1-yl)sulfonylpyrimidine-2,4(1H,3H)-dione

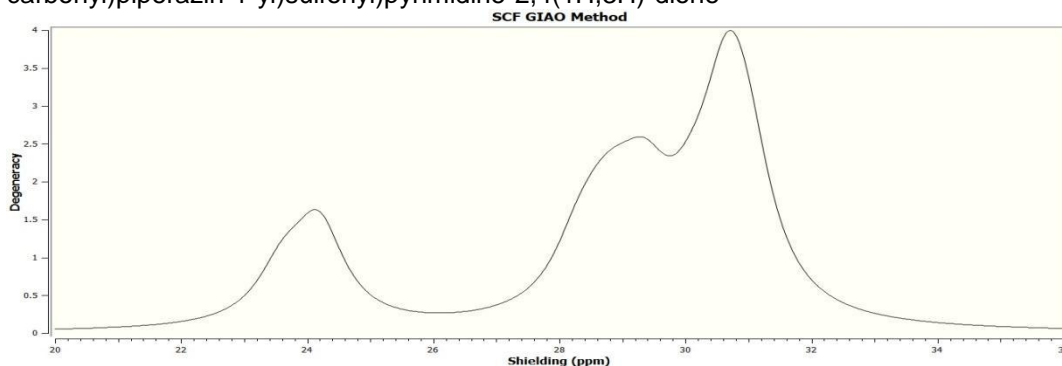


Fig. 10: Computational ^1H NMR spectra of N-butyl-N-methyl-2, 4-dioxo-1, 2, 3, 4-tetrahydropyrimidine-5-sulfonamide

UV – Visible Analysis: UV-vis evaluation Time-Dependent DFT computations are maximum outstanding and extensively hired in evaluation of digital spectra of molecules. In this study, the transitions from floor kingdom to excited kingdom are typically defined via way of means of one electron excitation among molecular orbitals. This calculation gives excited kingdom molecular geometry, absorption maxima (λ_{max}), oscillator strengths (f), excitation strength of the molecule [17]. The theoretical UV-Vis spectra on the DFT the usage of B3LYP 6-31 G+ (d, p), B3LYP 6-311 G+ (d, p) and TD-DFT the usage of B3LYP 6-311 G+ (d, p) foundation degree in DMSO as solvent (SMD model) as proven in Fig. eleven and 12.

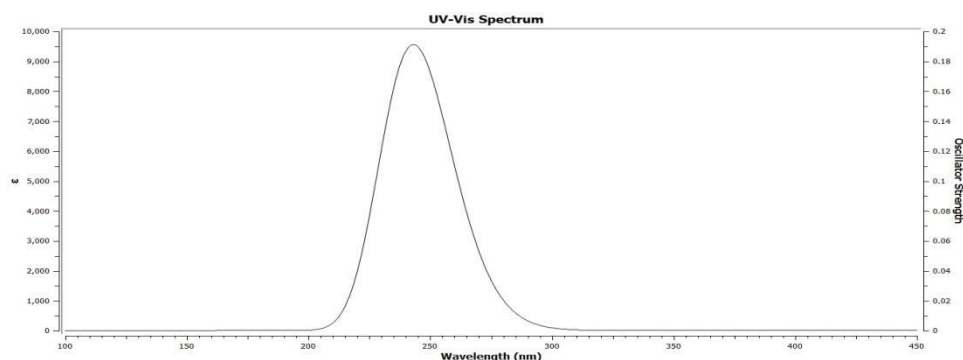


Fig. 11: Computational UV-Vis spectra of 5-(4-(2,3-dihydrobenzo[b][1,4]dioxine-2-carbonyl)piperazin-1-yl)sulfonylpyrimidine-2,4(1H,3H)-dione

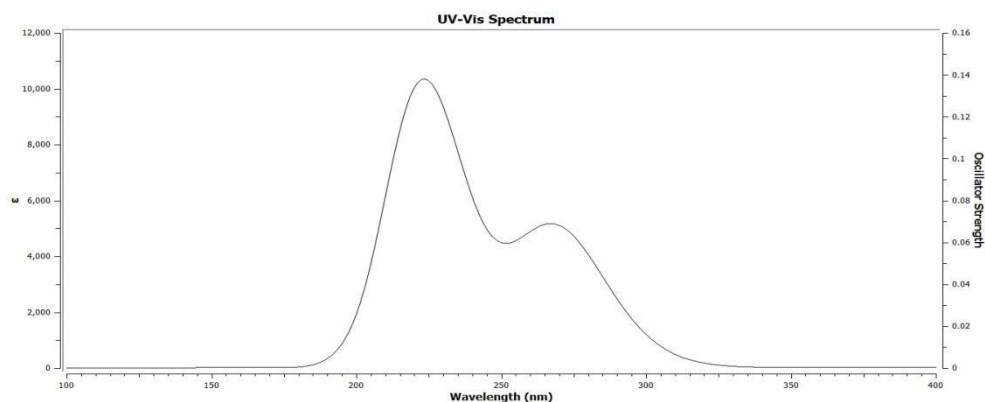
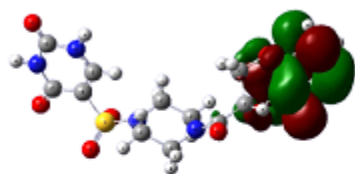


Fig. 12: Computational UV-Vis spectra of N-butyl-N-methyl-2, 4-dioxo-1, 2, 3, 4-tetrahydropyrimidine-5-sulfonamide

Frontier molecular orbital (FMO) studies: Energies and distributions of the FMO are very beneficial signs of the reactivity. The frontier molecular orbitals are the HOMO and the LUMO. HOMO represents the functionality to donate an electron and the LUMO represents the functionality to advantage an electron [18]. Energy hole among HOMO and LUMO orbitals represents a crucial parameter in figuring out and know-how molecular shipping properties. The three-D plots of HOMO-LUMO and (H-1) - (L+1) for compound Iis supplied in Fig. 13. EHOMO=-0.224 eV and ELUMO=-0.057eV are the energies of HOMO, LUMO and power hole is discovered to be 0.167 eV for compound I. EHOMO = -0.248 eV and ELUMO = -0.058 eV are the energies of HOMO, LUMO and power hole is discovered to be 0.189 eV and are supplied in Fig.14. Energy hole is taken into consideration to be reactivity indicator and for the reason that power hole price is under 1 eV, each the compounds may be taken into consideration as fairly solid molecules.

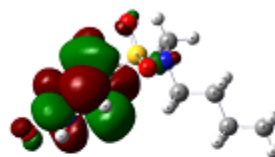
LUMO



$\Delta E = 0.16719$



LUMO



$\Delta E = 0.18998$



Fig. 13: Frontier molecular orbitals of 5-(4-(2,3-dihydrobenzo[b][1,4]dioxine-2-carbonyl)piperazin-1-yl)sulfonylpyrimidine-2,4(1H,3H)-dione

Fig. 14: Frontier molecular orbitals of N-butyl-N-methyl-2, 4-dioxo-1, 2, 3, 4-tetrahydropyrimidine-5-sulfonamide

pkCSM

It is a machine learning tool to predict the pharmacokinetic properties (ADMET) are calculated by using “pkCSM” of molecules. These parameters have been calculated and are summarized in Table 9.

pkCSM (ADMET)	5-(4-(2,3-dihydrobenzo[b][1,4]dioxine-2-carbonyl)piperazin-1-yl)sulfonyl)pyrimidine-2,4(1H,3H)-dione	N-butyl-N-methyl-2, 4-dioxo-1, 2, 3,4-tetrahydropyrimidine-5-sulfonamide
Water solubility	-2.958	-2.817
Caco2 permeability	0.669	-0.036
Intestinal absorption (human)	68.255	61.512
BBB permeability	-1.021	-0.525
CNS permeability	-3.338	-3.209
AMES toxicity	No	No
Max. tolerated dose (human)	0.284	1.082
Oral Rat Acute Toxicity (LD50)	1.758	1.799
Oral Rat Chronic Toxicity (LOAEL)	2.354	2.052
T.Pyriformis toxicity	0.287	0.077
LogP	-1.2639	-0.5162

SwissADME

“SwissADME” a web tool used to predict physicochemical properties, pharmacokinetics, Lipophilicity and drug-likeness among which in-house proficient methods such as the iLOGP and Bioavailability score. These parameters have been calculated and are summarized in Table 10.

Properties	5-(4-(2,3-dihydrobenzo[b][1,4]dioxine-2-carbonyl)piperazin-1-yl)sulfonyl)pyrimidine-2,4(1H,3H)-dione	N-butyl-N-methyl-2, 4-dioxo-1, 2, 3, 4-tetrahydropyrimidine-5-sulfonamide
iLOGP	1.85	0.85
XLOGP3	-0.87	-0.36
WLOGP	-0.94	0.56
MLOGP	-0.83	-0.53
ESOL Class	Very soluble	Very soluble
Ali Class	-1.8	-1.52
GI absorption	Low	High
log Kp (cm/s)	-9.49	-8.15
Lipinski #violations	1	0
Ghose #violations	1	0
Veber #violations	1	0
Egan #violations	1	0
Muegge #violations	1	0
Bioavailability Score	0.55	0.55

ChemAxon

Chemaxon is used to predict logP values and other structural properties. These parameters have been calculated and are summarized in Table 11.

Properties	5-(4-(2,3-dihydrobenzo[b][1,4]dioxine-2-carbonyl)piperazin-1-yl)sulfonyl)pyrimidine-2,4(1H,3H)-dione	N-butyl-N-methyl-2, 4-dioxo-1, 2, 3, 4-tetrahydropyrimidine-5-sulfonamide
Lipinski's rule of five	TRUE	TRUE
Topological polar surface area	134.35	95.58
Polarizability	38.72 A3	24.24 A3
Molar refractivity	98.43 cm ³ /mol	61.78 cm ³ /mol

REFERENCES

1. Hilly M, Adams ML, Nelson SC. A study of digit fusion in the mouse embryo. Clin Exp Allergy. 2002;32(4):489-98.
1. Heidelberger Charles, K. Chaudhuri, peter danneberg, dorothy mooren, lois griesbach, robert duschinsky, J. Schnitzer, Plevan & j. Scheiner.; fluorinated pyrimidines, a new class of tumor-inhibitory compounds. Nature. 1957; 179, 663-666.
2. B Venkata Sasidhar, Ph.D. thesis, GITAM (Deemed to be University), 2015.
3. M.J. Frisch, G.W. Trucks, H.B. Schlegel, G.E. Scuseria, M.A. Robb, J.R. Cheeseman, J.A. Montgomery Jr, T. Vreven, K.N. Kudin, J.C. Burant, J.M. Millam, S.S. Iyengar, J. Tomasi, V. Barone, B. Mennucci, M. Cossi, G. Scalmani, N. Rega, G.A. Petersson, H. Nakatsuji, M. Hada, M. Ehara, K. Toyota, R. Fukuda, J. Hasegawa, M. Ishida, T. Nakajima, Y. o, J. Jaramillo, R. Gomperts, R.E. Stratmann, O. Yazyev, A.J. Austin, R. Cammi, C. Pomelli, J.W. Ochterski, P.Y. Ayala, K. J Morokuma, A. Voth, P. Salvador, J.J. Dannenberg, V.G. Zakrzewski, S. Dapprich, A.D. Daniels, M.C. Strain, O. Farkas, D.K. Malick, A.D. Rabuck, K. Raghavachari, J.B. Foresman, J.V. Ortiz, Q. Cui, A.G. Baboul, S. Clifford, J. CioslHonda, O. Kitao, H. Nakai, M. Klene, X. Li, J.E. Knox, H.P. Hratchian, J.B. Cross, C. Adamowski, B.B. Stefanov, G. Liu, A. Liashenko, P. Piskorz, I. Komaromi, R.L. Martin, D.J. Fox, T.Keith, M.A. Al-Laham, C.Y. Peng, A. Nanayakkara, M. Challacombe, P.M.W. Gill, B. Johnson, W. Chen, M.W. Wong, C. Gonzalez, J.A. Pople, Gaussian Inc., Wallingford, CT, 2004.
4. A. Frish, A.B. Nielsen, A.J. Holder, GAUSSVIEW User Manual, Gaussian Inc., Pittsburg, PA, 2001.
5. Ajmal R Bhat1*, Rajendra S Dongre2 and Pervaz A Ganiel1, Petra, Osiris and Molinspiration: A Computational Bioinformatic Platform for Experimental in vitro Antibacterial Activity of Annulated Uracil Derivatives. Quarterly Journal of Iranian Chemical Communication.2018; 6,114-124.
6. S. Shefrin, Asha Asokan Manakadan, T. S. Saranya. A Computational study of anticancer activity of curcumin derivatives using in silico drug designing and molecular docking tools. Asian Journal of Chemistry. 2018; 30, 1335-1339.
7. Douglas E. V. Pires, Tom L. Blundell and David B. Ascher, pkCSM: predicting small-molecule pharmacokinetic properties using graph-based signatures. J. Med. Chem. 2015; 58, 4066-4072.
8. Antoine Daina, Olivier Michielin, Vincent Zoete1, SwissADME: a free web tool to evaluate pharmacokinetics, druglikeness and medicinal chemistry friendliness of small molecules. Scientific reports-nature, 2017; Article number 42717.

9. Arnott, J. A. & Planey, S. L. The influence of lipophilicity in drug discovery and design. *Expert Opin. Drug Discov.* 2012; 7, 863–875.
10. Kamel Mansouri¹, Neal F. Cariello, Alexandru Korotcov, Valery Tkachenko, Chris M. Grulke, Catherine S. Sprankle, David Allen, Warren M. Casey, Nicole C. Kleinstreuer and Antony J. Williams. *Journal of Cheminformatics*, 2019.
11. Muthu, Sambanthan & Maheswari, J. (2012). Quantum mechanical study and spectroscopic (FT-IR, FT-Raman, C-13, H-1, UV) study, first order hyperpolarizability, NBO analysis, HOMO and LUMO analysis of 4-[(4-aminobenzene) sulfonyl] aniline by ab initio HF and density functional method. *Spectrochimica Acta. Part A, Molecular and biomolecular spectroscopy*. 92. 154-63. 10.1016/j.saa.2012.02.056.
12. Fritzsche, Hartmut. (2010). *Vibrational spectra of benzene derivatives: Von G. Varsányi. Akadémiai Kiadó, Budapest. 1969, 430 Seiten mit zahlreichen Bildern und Tabellen, Format 16, 5 × 23 cm, Ln. Zeitschrift für Chemie.* 10. 10.1002/zfch.19700100626.
13. H. Pir, N. Gunay, O. Tamer, D. Avci, Y. Atalay, Theoretical investigation of 5-(2-Acetoxyethyl)-6-methylpyrimidin-2,4-dione: conformational study, NBO and NLO analysis, molecular structure and NMR spectra, *Spectrochim. Acta.* 2013; Part A 112, 331-342.
14. L.D.S. Yadav, *Organic Spectroscopy*, Anamaya Publishers, New Delhi, India, 2005.
15. V. Balachandran, S. Rajeswari, S. Lalitha, DFT computations, vibrational spectra, monomer, dimer, NBO and NMR analyses of antifungal agent: 3,5- Dibromosalicylic acid, *J. Mol. Struct.* 2012; 1007, 63-73.
16. F. Bardak, C. Karaca, S. Bilgili, A. Atac, T. Mavis, A.M. Asiri, M. Karabacak, E. Kose, Conformational, electronic, and spectroscopic characterization of isophthalic acid (monomer and dimer structures) experimentally and by DFT, *Spectrochim. Acta.* 2016; Part A 165, 33e46.
17. M. Arivazhagan, D. Anitha Rexalin, Vibrational spectra, UV-vis spectral analysis and HOMO-LUMO studies of 2,4-dichloro-5-nitropyrimidine and 4-methyl-2-(methylthio)pyrimidine, *Spectrochimica Acta Part A: Molecular and Biomolecular Spectroscopy.* 2013; 107, 347-358.
18. Sudhir M. Hiremath, A. Suvitha, Ninganagouda R. Patil, Chidanandayya, S. Hiremath, Seema S. Khemalpure, Subrat K. Pattanayak, Veerabhadrayya, S. Negalurmah, Kotresh Obelannavar, J. Sanja, Stevan Armakovi, Armakovi, Synthesis of 5-(5-methylbenzofuran-3-ylmethyl)-3H-[1, 3, 4] oxadiazole-2-thione and investigation of its spectroscopic, reactivity, optoelectronic and drug likeness properties by combined computational and experimental approach, *Spectrochim. Acta.* 2018; Part A 205, 95-110.